Low dimensional flow control using Galerkin POD

Ying Wang and Günter Bärwolff

Technische Universität Berlin, Institut für Mathematik

Abstract. An aspect of recent developments in computational methods for control of fluids is the design of reduced-order controllers, for reducing the CPU costs of flow solves. In this paper a reduced order approach will be introduced for the optimal boundary control problem governed by the unsteady Navier Stokes equations with the help of the Galerkin proper orthogonal decomposition(POD) method. The paper summarizes the results of the diploma-thesis [Wang2008].

The Galerkin Proper orthogonal decomposition provides a method for deriving reduced order models of dynamical systems. It's based on projecting the dynamical system onto subspaces of snapshots ensemble, which is composed of the solutions for the physical system at pre-specified time instances or experimental measurements. These snapshots are not suitable as the basis for the ensemble spanned by themselves by reason of the possible linear dependence. We will find the orthogonal basis for the ensemble by solving an eigenvalue problem, and these basis will be denoted in the thesis as POD basis, and number of these POD basis can be very small in comparison with the number of the snapshots. The POD basis spanned subspace is just that, which the dynamical system will be projected onto.

The goals of the paper are at first applying the POD basis to simulate the original flow in two dimensional rectangle. We hope that in this manner the POD method can reduce the computational cost of the nonlinear flow solutions. Moreover, a boundary condition should be found, so that the unsteady Navier Stokes equations is solved with this boundary condition and meanwhile its solution minimized dynamically an extra cost functional, which contains the state and the control variable. In this optimization procedure we continue with the help of POD basis to derive an optimal control system for the reduced order models. POD-based optimization is going to work, only if the snapshots contains enough information to model all the dynamical behavior of the flows that are encountered throughout the optimization process.

Keywords: Navier-Stokes equation, incompressible flow, optimization, flow control
PACS: 45.70.Vn, 47.10.ad, 47.11.-j, 47.11.Df, 47.85.L-

THE DESCRIPTION OF THE METHOD

Firstly we concentrate ourself on the snapshots ensemble, the FVM method discretization and Newton iteration are applied for the snapshots of the 2-dimensional rectangle dynamical system, which is described by the following Navier Stokes equations. boundary.

$$\begin{aligned}
\mathbf{y}_t - \frac{1}{Re}\Delta\mathbf{y} + \mathbf{y}\cdot\nabla\mathbf{y} + \nabla p = 0 \qquad & \text{in } Q \\
\nabla\cdot\mathbf{y} = 0 \qquad & \text{in } Q \\
\mathbf{y}(\mathbf{x},0) = \mathbf{y}_0(\mathbf{x}) \qquad & \text{in } \Omega \\
p\nu - \frac{1}{Re}\frac{\partial\mathbf{y}}{\partial\nu} = (0,0) \qquad & \text{on } \Sigma_{out} \\
\mathbf{y}(\mathbf{x},t) = u(t)\cdot\mathbf{g}(\mathbf{x}) \qquad & \text{on } \Sigma_{in} \\
\mathbf{y}(\mathbf{x},t) = (0,0) \qquad & \text{on } \Sigma_{wall}
\end{aligned}$$

We study the theory of the Galerkin Proper Orthogonal Decomposition through understanding, finding and using the POD. For understanding POD we discuss the finite and infinite case and with a convergence statement to combine the both cases. By minimizing a least square formula error, one finds the POD basis system as the global optimal solution of it in the snapshots ensemble. Meanwhile the Singular Value Decomposition is also very helpful to understand how to find the orthogonal POD basis, and its algorithm is detailed. With the numerical experiment the six POD basis and two extra POD basis could simulate almost the spatial behavior of two hundreds snapshots, and they take the almost full order kinetic energy of the dynamical snapshots.

One application of the POD basis is to simulate the original flow with the combination of the POD basis and Galerkin weak formulation. We project the above Navier Stokes equation on the POD subspace, which is spanned by POD basis, develop the original solution of Navier Stokes equation with respect to the total eight POD basis, then yields

$$\begin{cases} \dot{\mathbf{X}}(t) = \begin{pmatrix} 1' \\ \beta'(t) \\ c'(t) \end{pmatrix} = \begin{pmatrix} 0 \\ -\frac{1}{Re} A\,\mathbf{X}(t) - K(\mathbf{X}(t)) \\ 0 \end{pmatrix} + \mathrm{u}(t) \begin{pmatrix} 0 \\ Bv \\ 1 \end{pmatrix} \\ \mathbf{X}(0) = \begin{pmatrix} 1 \\ \beta(0) \\ c_0 \end{pmatrix}, \text{ where } \quad \beta(0) = \begin{pmatrix} \langle \mathbf{y}_0 - \mathbf{y}_m - c_0 \mathbf{y}_c, \Phi_1 \rangle_{L^2(\Omega)^2} \\ \vdots \\ \langle \mathbf{y}_0 - \mathbf{y}_m - c_0 \mathbf{y}_c, \Phi_M \rangle_{L^2(\Omega)^2} \end{pmatrix} \end{cases}$$

The simulation of fluid flow can be completed by solving the above nonlinear ODE system. The numerical example shows that the advantage of the POD reduced order models is not only the dynamical system can be solved simply, reliably and quickly but also the strong short term simulation capacity.

An an acquaintance the boundary optimal control for Navier Stokes equations (P_d) is introduced in the thesis and its first order optimality obtained with an Attempt of the Lagrange formal technique but numerical difficult to execute.

$$(P_d) \qquad \begin{aligned} \min J(\mathbf{y},u) = \frac{1}{2}\int_0^T \|y(t,.) - y_d\|_H^2 dt + \frac{\sigma}{2}\int_0^T \quad u^2(t) \quad dt \\ \text{subject to:} \quad \mathbf{y}_t - \frac{1}{Re}\Delta\mathbf{y} + \mathbf{y}\cdot\nabla\mathbf{y} + \nabla p = 0 \qquad \text{in } Q \\ \nabla\cdot\mathbf{y} = 0 \qquad \text{in } Q \\ \mathbf{y}(\mathbf{x},0) = \mathbf{y}_0(\mathbf{x}) \qquad \text{in } \Omega \\ p\nu - \frac{1}{Re}\frac{\partial\mathbf{y}}{\partial\nu} = (0,0) \qquad \text{on } \Sigma_{out} \\ \mathbf{y}(\mathbf{x},t) = u(t)\cdot\mathbf{g}(\mathbf{x}) \qquad \text{on } \Sigma_{in} \\ \mathbf{y}(\mathbf{x},t) = (0,0) \qquad \text{on } \Sigma_{wall} \end{aligned}$$

Then alternatively the penalized Neumann boundary control for Navier Stokes equations $(P_{n\varepsilon})$ can be presented to avoid the numerical difficulty of (P_d), which differs from the control problem (P_d) only on the inflow boundary condition.

$$p\nu - \frac{1}{Re}\frac{\partial\mathbf{y}}{\partial\nu} + \frac{1}{\varepsilon}\mathbf{y}(\mathbf{x},t) = \frac{1}{\varepsilon}u(t)\cdot\mathbf{g}(\mathbf{x}) \qquad \text{on } \Sigma_{in}$$

Under certain assumptions, the optimal solution of $(P_{n\varepsilon})$ converges strongly in $L^2(0,T)$ to the solution of (P_d), as $\varepsilon \to 0$.

Another application of the POD basis is POD approach to the optimal boundary control for Navier Stokes equations. In the simulation stage it is possible that in POD subspace a satisfying solution of NSE can be found. Equally the largest projection of the cost functional should be also considered in the POD subspace. Then the optimal boundary problem subjects to the Navier Stokes equations can be converted to the POD boundary control problem (P_M), whose cost functional with respect to POD basis subjects to the above nonlinear ODE as state equation.

$$(P_M) \begin{cases} \min J(\mathbf{X}(t),u(t)) = \frac{1}{2}\int_0^T \Big[(\mathbf{X}(t)-\mathbf{X}_d)^T\cdot\Psi\cdot(\mathbf{X}(t)-\mathbf{X}_d) + \sigma\mathrm{u}^2(t)\Big]dt \\ \text{subject to:} \\ \qquad \mathbf{X}'(t) = \vec{F}(\mathbf{X}) + \mathrm{u}(t)B \\ \qquad \mathbf{X}(0) = \mathbf{X}_0 \end{cases}$$

The existence optimal control solution of (P_M) is proved under some assumptions and for the first order optimality condition with Pontryagin Maximum Principle and weak Minimum Principle we could get the following system

$$\text{state equation} \Rightarrow \begin{cases} \dot{\mathbf{X}}(t) = \vec{F}(\mathbf{X}) + \mathrm{u}(t) \cdot B \\ \mathbf{X}(t_0) = \mathbf{X}_0 \end{cases}$$

$$\text{adjoint equations} \Rightarrow \begin{cases} -\dot{w} = \left[f_0\right]_{\mathbf{X}} + \left[\vec{F}\right]_{\mathbf{X}}^T w \\ w(T) = 0 \end{cases}$$

$$\text{variation inequality} \Rightarrow \begin{cases} \int_0^T (\sigma \mathrm{u}^* + B^T w)(\mathrm{u} - \mathrm{u}^*) dt \geq 0 \qquad \forall \mathrm{u} \in \mathscr{U}_{ad} \end{cases}$$

The optimality system can be solved by in the thesis formulated algorithm combined with CG method and Armijo step size control. One solves once nonlinear state ODE and once linear adjoint ODE in every control iterative step instead of for the optimal control problem subjects to semi-linear partial differential equation to solve expensively once semi-linear parabolic PDE and once linear parabolic PDE in every iterative step. That is why recently much more attention has been paid to reducing the costs of the nonlinear flow control problem by using reduced order models for the flow. We set now the optimal solution of (P_M) as the controlled configuration in the Navier Stokes equations Solver to calculate the controlled flow. The result shows the successful controls are captured with respect to the different σ values, which minimizes the cost functional and reduces the extra vortex of the original flow.

RESULTS OF NUMERICAL EXPERIMENTS

Here we will illustrate the numerical experiments result of the POD approach in solving the boundary flow control problem.

For snapshots we use the same configuration as in the simulation stage. That means the linear profile for $c(t)$ was taken and consequently the start guess u_0 must be constant, which strongly depends on the choice of $c(t)$, since it must hold $c'(t) = u(t)$. Hereby two hundreds snapshots as many as in the POD simulation were be recorded. The eigenvalues of the correlation matrix in Fig 1, which is generated from the controlled solution of Navier Stokes equations as the renewed snapshots set, decay rapidly and the most eigenvalues are clearly smaller than these in the uncontrolled case. The percentage of the controlled fluid dynamics energy capture by the new calculated POD basis are given in Table 1, as before 6 POD basis carry the 99.9999% kinetic energy.

TABLE 1. % of controlled full order model energy captured with $M = 1, ..., 6$

M	1	2	3	4	5	6
Energy in %	89.1467	95.4803	99.7010	99.9893	99.9997	99.9999

The penalty parameter σ is found to play a critical role in the controller design. In Fig 2 we present the $u(t)$ in POD system and $c(t)$ in the NSE system at different σ values. The relative smaller value of σ can more quickly bring the flow state to the expected one, but relative too large σ value couldn't bring the enough satisfied flow and too small causes to the oscillation. With value $\sigma = \frac{1}{20}$, a smooth control was obtained. Here we mention the optimal steady flow doesn't belong to the snapshots, that is to say, there exists error, if one projects this steady flow onto the POD subspace. Consequently it results in unaccomplished control missions with some σ values.

In Fig 3 the cost functional curve shows the convergence to the local minimum with respect to the iteration number. The expression $\sigma \mathrm{u}^*(t) + B^T w(t)$ is evaluated and shown in the Table 2 regarding the supremum norm, which displays the descent direction almost zero, consequently the corresponding convergence solutions u^* are local optimal for different σ values.

TABLE 2. Estimation of the descent direction of the CG algorithm

σ	0.1	0.05	0.01	0.001
$\|\sigma \mathrm{u}_n(t) + B^T w(t)\|_{C(0,T)}$	$1.9901e-08$	$3.2144e-08$	$7.6844e-07$	$3.4349e-07$

The flow fields presented in Fig 4 - Fig 5 are flow profiles at different stations for the controlled and uncontrolled cases at $t = 4$, $t = 7$ and $t = 10$. We could simply read the difference between snapshots profile and POD boundary controlled flow profile. At $t = 4$ the difference was not large, by and by POD controlled flow profile was flinching because of the reduced inflow, such that the forth vortex was successfully avoided.

For giving a clear sight for reducing the forth vortex, in Fig 6 - Fig 7 demonstrate the both streamlines, in which we confirm that in uncontrolled flow appeared vortex in the left above wall corner vanishes, because an expected flow is set in the objective functional at the pattern flow, which has no vortex. In Fig 7 we could read at $t = 7$ the uncontrolled flow has the tendency that the forth vortex on the left above corner is arising, and at $t = 10$ it finished. But the controlled flow is stiller than the uncontrolled one as expected, and from beginning to end the forth vortex didn't arise.

The steady pattern flow is presented in Fig 8, inclusive the flow velocity demonstration and streamline.

ACKNOWLEDGMENTS

We acknowledge support and useful discussion with Prof. Dr. Fredi Tröltzsch (TU Berlin).

REFERENCES

Wang2008. Ying Wang. Reduced Order Optimal Control for Fluid Flows by Using Galerkin POD. *Diploma thesis*, TU Berlin, 2008.

Al96. A. Allievi and R. Bermejo. A Generalized Particle Search-Locate Algorithm for Arbitrary Grids. *Journal of computational physics*, 132: 157-166, 1997.

Al99. H.W. Alt. *Lineare Funktionalanalysis*. Springer, Berlin, 1999.

Al02. W. Alt. *Nichtlineare Optimierung*. Vieweg, 2002.

Bä88. G. Bärwolff. Numerische Berechnung von Transportprozessen fluider medien. *Report des Zentrums für wissenschaftlichen Gerätebau der Akademie der Wissenschaften der DDR*, Berlin, 1988.

Em04. E. Emmrich. *Gewöhnliche und Operator-Differentialgleichungen*. Vieweg, 2004

Fa01. M. Fahl. Computations of POD Basis Functions for Fluid Flows with Lanczos Methods. *Mathematical and Computer Modelling*, 34: 91-107, 2001.

Gr97. M. Griebel, T. Dornseifer and T. Neunhoeffer. *Numerical simulation in Fluid Dynamics a pratical introduction*. SIAM. 1997.

Hi04. M. Hinze and K. Kunisch. Second order methods for boundary control of the instationary Navier-Stokes system. *ZAMM*, 84: 171-187, 2004.

Ho98. L. S. Hou and S. Ravindran. A penalized Neumann control approach for solving an optimal Dirichlet control problem for the Navier-Stokes equations. *SIAM J. Control Optimization*, 36: 1795-1814, 1998.

Ku02. K. Kunisch and S. Volkwein. Galerkin proper orthogonal decomposition methods for a general equation in fluid dynamics. *SIAM J. Numer. Anal.*, 40: 492-515, 2002.

Pi93. E. R. Pinch. *Optimal control and the Calculus of Variations*. Oxford University Press, 1993.

Ra00. S. Ravindran. A reduced order approach to optimal control of fluids using proper orthogonal decomposition. *Int. J. Numer. Methods Fluids*, 34(5): 425-448, 2000.

Ra00. S. S. Ravindran. Reduced-Order Adaptive Controllers for Fluid Flows Using POD. *J. Sci. Comput.*, 15(4): 457-478, 2000.

Sa94. R.L. Sani and P.M. Gresho. Resume and remarks on the open boundary condition mini-symposium. *International Joundal of Numerical Methods in Fluids.* 18: 983-1008, 1994.

Tr07. F. Tröltzsch and S. Volkwein. POD a-posterior error estimates for linear-quadratic optimal control problems. *Computional Optimization and Applications*, to apprear.

Tr05. F. Tröltzsch. *Optimale Steuerung partieller Differentialgleichungen*. Vieweg, Berlin, 2005.

Vo06. W. Vogt. Adaptive Verfahren zur numerischen Quadratur und Kubatur. *Preprint No. M 1/06, IfMath TU Ilmenau*, 2006.

Vo99. S. Volkwein. Proper orthogonal decomposition and singular value decomposition. *SFB-Preprint No. 153*, 1999.

Vo01. S. Volkwein. Optimal Control of a Phase-Field Model Using Proper Orthogonal Decomposition. *ZAMM. Z. Angew. Math. Mech.*, 81(2): 83-97, 2001.

Wa06. D. Wachsmuth. *Optimal control of the unsteady Navier-Stokes equations*. Dissertation, 2006.

We95. D.Werner. *Funktionalanalysis*. Springer, 1995

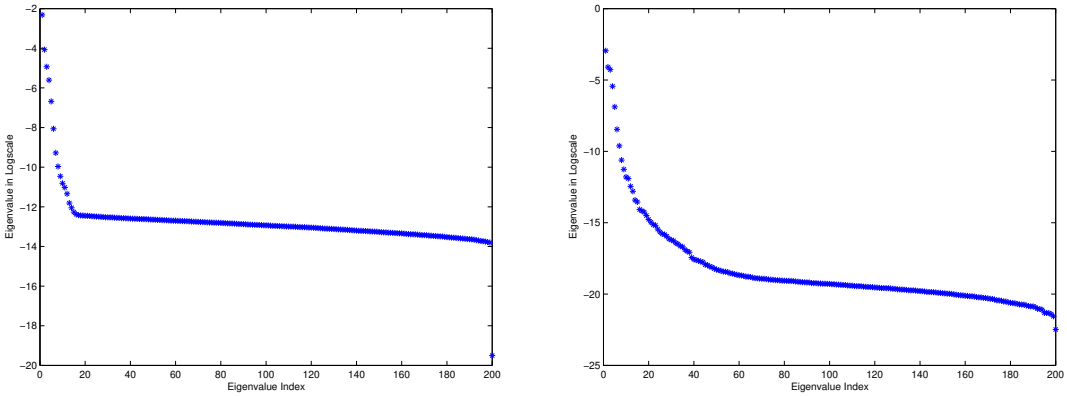

FIGURE 1. Eigenvalues of the correlation matrix for baseline and controlled case

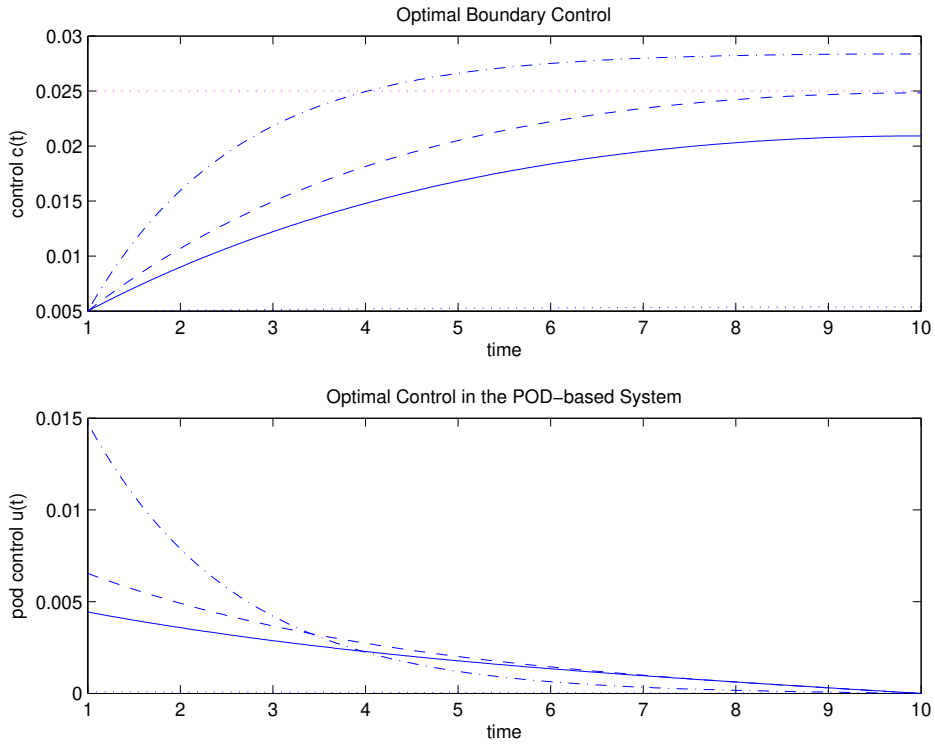

FIGURE 2. Optimal boundary control of NSE and POD-based system for different values of sigma: 10(dotted line), $1/10$(solid line), $1/20$(dashed line), $1/100$(dash-dot line) and expected boundary profile (magenta dotted line)

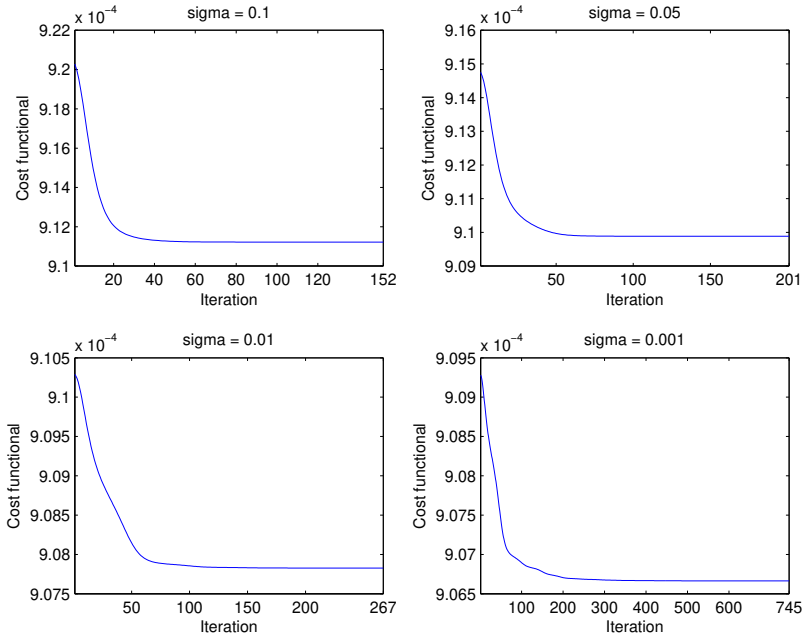

FIGURE 3. The cost functional curve.

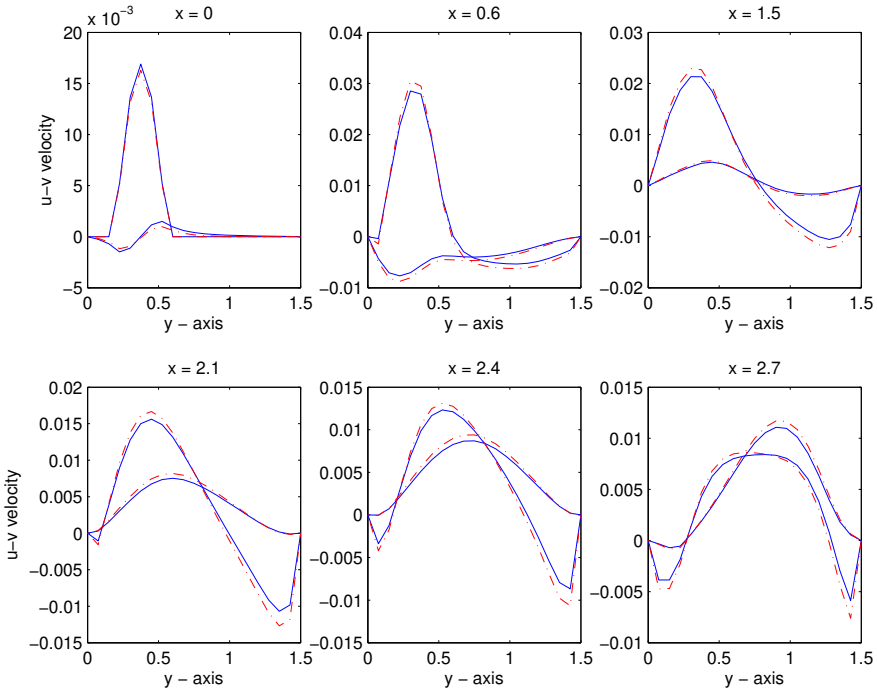

FIGURE 4. Controlled(red dashed dot line) and uncontrolled(blue solid line) flow profile comparison at various situations in $t = 4$.

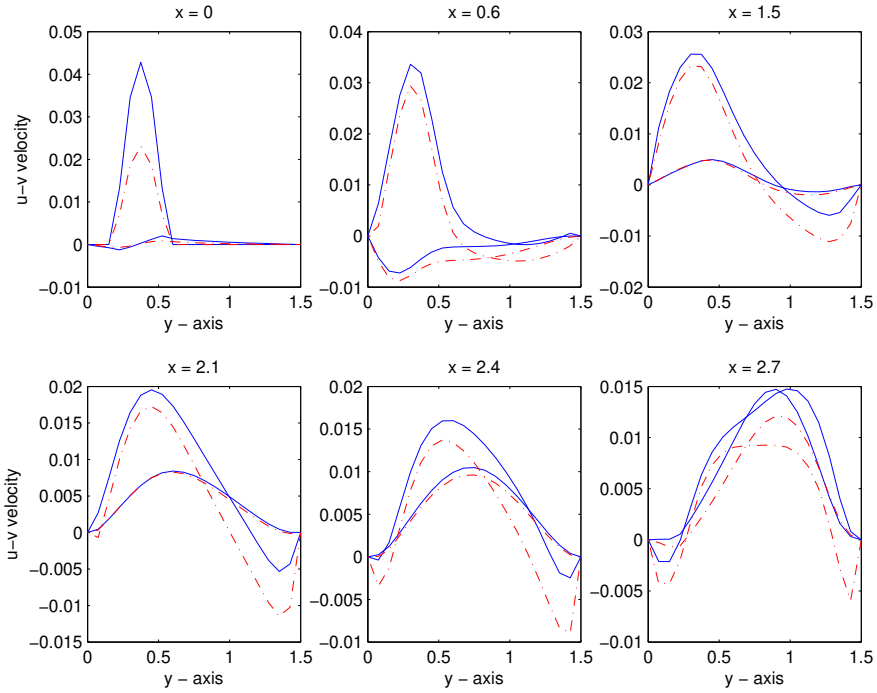

FIGURE 5. Controlled(red dashed dot line) and uncontrolled(blue solid line) flow profile comparison at various situations in $t = 10$.

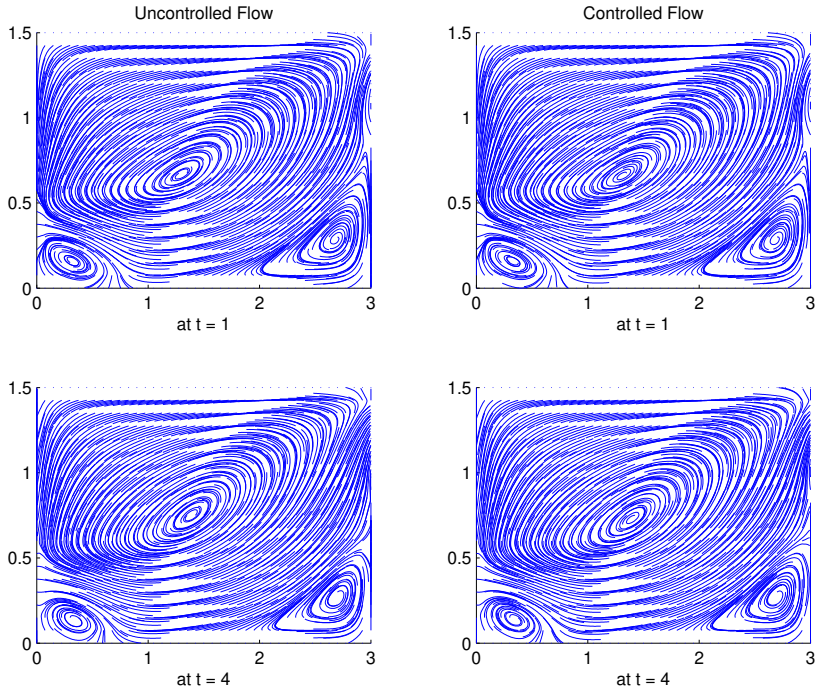

FIGURE 6. Controlled and uncontrolled flow streamline comparison in $t = 1$ and $t = 4$.

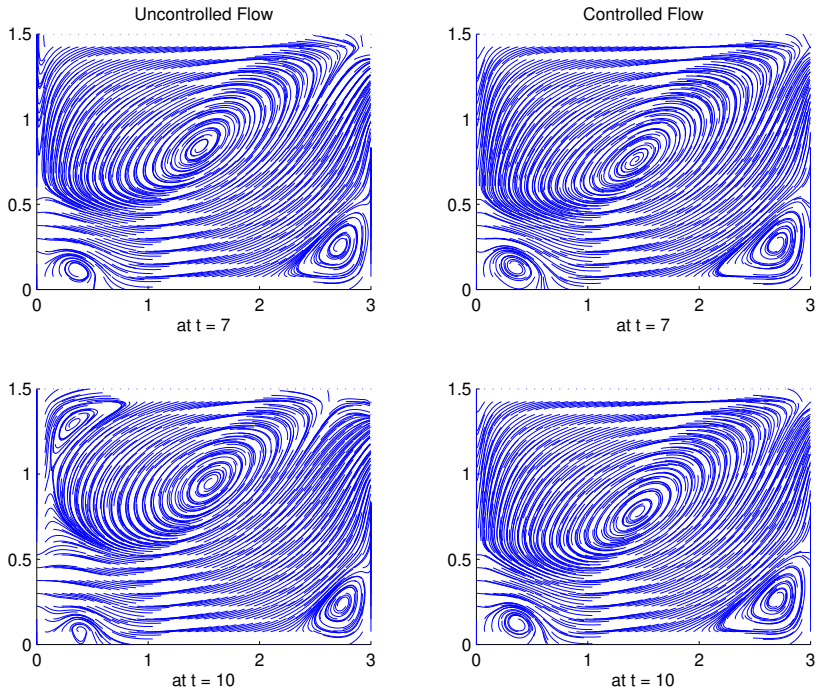

FIGURE 7. Controlled and uncontrolled flow streamline comparison in $t = 7$ and $t = 10$.

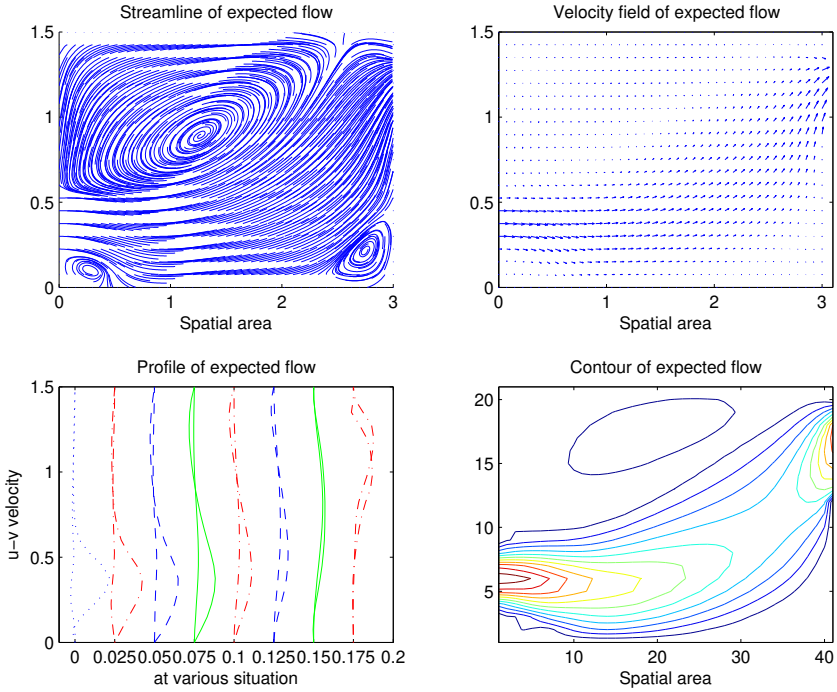

FIGURE 8. The steady pattern flow with $c(t) = 0.025$.